Optical-force laws for guided light in linear media

Thales Fernando Damasceno Fernandes

Universidade Federal de Minas Gerais, Physics Department, 30123-970 Belo Horizonte, Minas Gerais, Brazil
and Centro de Desenvolvimento da Tecnologia Nuclear–CDTN/CNEN, Avenida Presidente Antônio Carlos, 6.627 Belo Horizonte,
Minas Gerais, Brazil

Pierre-Louis de Assis[*]

"Gleb Wataghin" Institute of Physics, University of Campinas–UNICAMP, Department of Applied Physics,
13083-859 Campinas, São Paulo, Brazil

The mechanical response of transparent materials to optical forces is a topic that concerns a wide range of fields, from the manipulation of biological material by optical tweezers to the design of nano-optomechanical systems. However, the fundamental aspects of such forces have always been surrounded by controversies, and several different formulations have been proposed. In this paper, we propose a general stress tensor formalism to put all optical forces in a consistent presentation that allows us to study how different predictions emerge, and use the specific case of light propagating as a superposition of guided modes in lossless dielectric waveguides as a physical example. We use this formalism to calculate optical forces for straight and curved waveguide sections and all possible excitation configurations for a given set of coupled eigenmodes, and then compare the results for each of the known proposed optical-force laws in a framework that permits distinguishing where there will be differences between the force laws proposed. The general formalism also allows us to show that proper use of the divergence theorem is crucial to account for all force terms, many of which vanish if the procedure most commonly used is applied for situations other than eigenmodes in straight waveguides in vacuum. Finally, it is known that discrepancies in the predicted forces arise from the incompleteness of each stress tensor with respect to the total-energy-momentum tensor of the system. A better understanding of how different stress tensors predict very different forces for certain waveguide geometries should open a pathway to identifying how to properly assemble the full tensor, as well as for experimental tests to confirm the predictions.

I. INTRODUCTION

It has been known since Maxwell that electromagnetic waves carry momentum and can exert forces on material objects when reflected, refracted, or absorbed [1]. Mechanical interactions between light and matter have been developed into applications that range from atomic cooling [2] to micro-optomechanical devices and the manipulation of living cells using optical tweezers [3–5].

For all the applications already developed, however, there are still points in the theory of optical forces that are open to discussion. The most well known is the Abraham-Minkowski controversy about how to properly define the momentum of light in dielectric media [6–8]. Less known is the multitude of proposed force laws or methods to calculate the optical force [9–13], which may agree in certain situations while disagreeing in others [8].

As discussed in [5], even though the Abraham-Minkowski controversy is well known, the fact that a part of the optical-force community considers that a consensus has been reached is not. This consensus is that the Minkowski stress tensor represents an incomplete picture of the light-matter system,

a problem shared by all other tensors proposed when trying to correct the lack of symmetry in the Minkowski tensor. While there should exist a single total-energy-momentum tensor for each system, which predicts the correct mechanical effects of light-matter interactions, obtaining such a tensor is not trivial. Therefore, given the variety of stress tensor and optical-force law propositions existing in the literature, it is useful to have a common framework upon which to build a clear understanding of how and when differences arise between the predictions of each optical-force law.

In order to compare the different proposed optical-force laws in a way that allows us to discern the reasons for their disagreements in certain conditions and agreements in others, we have chosen to focus our paper on a simple, yet enlightening, system composed of a pair of nonmagnetic linear lossless dielectric waveguides in close proximity, so as to be evanescently coupled. By studying the stationary regime of light propagation and considering static waveguides, we are able to isolate the optical-force analysis from the context of more complex phenomena such as photon-phonon interactions [14,15], especially Brillouin scattering [16,17]. While the forces studied in our paper may provide an interaction pathway for Brillouin scattering in certain photonic devices, that is not within the scope of our investigation. Our choice of constraints also sets the optical forces under study apart from

_____
[*]plouis@ifi.unicamp.br

electrostrictive effects, which are intrinsically dependent on deformations of the dielectric material [18].

In Sec. II we present the general stress tensor, from which we can obtain the known stress tensors by choosing two binary parameters, and discuss how the divergence theorem, when applied to a waveguide cross section, gives a general optical-force density. This force density can be dissected into three distinct contributions: one due to mode superposition, one due to waveguide curvature, and the more well-known term due to the global eigenmodes of the coupled system.

In Sec. III we first show numerical results for the force densities acting on a pair of coupled waveguides. We have simulated silicon waveguides in vacuum, with dimensions chosen so that they support two TE-like and two TM-like modes. For straight waveguides we present the x, y, and z components of the force density for each force law, in single eigenmode propagation as well as for all superpositions of the four modes. We use the general tensor formalism to discuss what physical insight can be gained from comparing how some force laws agree for some components and disagree for others, and how this relates to the broader picture of the Abraham-Minkowski discussion. We then briefly proceed to discuss the more complex force term arising from a curvature in the waveguide pair, going from two parallel waveguides to two sections of concentric rings. In this scenario all force laws disagree even in the simplest case of single-eigenmode forces.

II. GENERAL TENSOR FORMULATION

The momentum balance in an electromagnetic system can be cast in a simple form as [19]

$$\mathcal{F} + \partial_t \mathcal{G} = \nabla \cdot \mathcal{T}, \tag{1}$$

where t is the time, $\mathcal{F}$ is the force density, $\mathcal{G}$ is the momentum density, and $\mathcal{T}$ is the stress tensor.

Let $\mathcal{T}_{nm}$ be the general stress tensor defined as

$$\mathcal{T}_{nm} = \varepsilon_0 \big(\varepsilon^n \mathcal{E} \otimes \mathcal{E} - \tfrac{1}{2} \varepsilon^m \mathcal{E} \cdot \mathcal{E} \big) + \mu_0 \big(\mathcal{H} \otimes \mathcal{H} - \tfrac{1}{2} \mathcal{H} \cdot \mathcal{H} \big), \tag{2}$$

where n and m can be either 0 or 1 and will be used to label different stress tensors; $\mathcal{E}$ and $\mathcal{H}$ are the time-dependent electric and magnetic fields, respectively; ε is the relative permittivity of the material, and $\mathbb{1}$ is the identity matrix. Henceforth it will be assumed the material is a nonmagnetic linear lossless dielectric and that the guided waves are monochromatic. With this general definition, we have that $\mathcal{T}_{00}$ is the Lorentz stress tensor [12,13]; $\mathcal{T}_{10}$ is the Einstein-Laub (E-L) stress tensor [12]; $\mathcal{T}_{11}$ is the Minkowski stress tensor, which for the linear dielectrics under consideration coincides with the Abraham stress tensor [12]; and $\mathcal{T}_{01}$ is a linear combination of the previous three stress tensors, not found in the literature. It is possible that $\mathcal{T}_{01}$ contains no new physics, being just a consequence of the definition of the general stress tensor, but as its three components are considered to be incomplete descriptions of the light-matter system—in different manners—we believe further investigation would be necessary to make this assertion.

Taking the divergence of the general stress tensor and using the momentum balance Eq. (1) we can define the following force densities [12,13]:

$$\mathcal{F}_{00} = -\mathcal{E}\nabla \cdot \mathcal{P} + \mu_0 \partial_t \mathcal{P} \times \mathcal{H}, \quad \text{Lorentz}, \tag{3}$$

$$\mathcal{F}_{10} = (\mathcal{P} \cdot \nabla)\mathcal{E} + \mu_0 \partial_t \mathcal{P} \times \mathcal{H}, \quad \text{Einstein-Laub}, \tag{4}$$

$$\mathcal{F}_{11} = -\tfrac{1}{2}\varepsilon_0 \mathcal{E} \cdot \mathcal{E}\nabla\varepsilon, \quad \text{Minkowski}, \tag{5}$$

$$\mathcal{F}_{01} = \mathcal{F}_{00} + \mathcal{F}_{11} - \mathcal{F}_{10}, \quad \text{unnamed}, \tag{6}$$

where $\mathcal{P} = \varepsilon_0(\varepsilon - 1)\mathcal{E}$ is the polarization density. It should be noted that the E-L force is also well known as the gradient force on an induced dipole.

Taking the time average of the momentum balance Eq. (1), we have

$$\langle \mathcal{F} \rangle + \underbrace{\langle \partial_t \mathcal{G} \rangle}_{=0} = \nabla \cdot \langle \mathcal{T} \rangle, \tag{7}$$

where $\langle \partial_t \mathcal{G} \rangle = 0$ comes from the time-averaging process of time-harmonic fields. For optical frequencies, such as the ones we consider in this paper, terms originated from the temporal variation of the electromagnetic momentum will not contribute to the time-averaged force $\langle \mathcal{F} \rangle$.

The force densities shown above are very different in form, even though they originate from quite similar stress tensors. While a comparison of their effects based solely on the examination of the formulations presented in Eqs. (3)–(6) is a complex task, we can indeed analyze their differences by calculating their effect on a model system composed of dielectric waveguides that are assumed to be perfectly rigid. This condition is reasonable for all time scales longer than the optical periods, typically in the femtoseconds, but still much shorter than those associated to acoustic responses of solids, which are no shorter than some nanoseconds. This allows us to examine the optical forces in a context that is free of other optomechanical effects such as electrostriction or photon-phonon scattering and study the regime of static deformations.

In order to facilitate calculations, we use the standard procedure of applying the divergence theorem to cast the total force in terms of a surface integral instead of the volume integral of a divergence. This avoids field derivatives altogether, which is particularly beneficial when using the finite elements method (FEM) in numerical simulations. The total force can be given by

$$\mathbf{F}_{\text{tot}} = \iiint_\Omega \nabla \cdot \langle \mathcal{T} \rangle dV = \iint_\Gamma \langle \mathcal{T}_{\text{out}} \rangle \cdot \hat{\mathbf{n}}\, dS, \tag{8}$$

where Ω is the volume of integration, Γ is its boundary, and $\hat{\mathbf{n}}$ is the outward normal unit vector. When using the divergence theorem for electromagnetic fields in dielectrics, one needs to take into account the discontinuity of the fields at the boundary and use the proper discontinuous form of the divergence theorem [20,21]. It can be shown that the fields to be taken into account in a discontinuous stress tensor are the fields outside the domain of integration ($\mathcal{T}_{\text{out}}$) [22].

In our model system of light propagating in coupled waveguides with rectangular cross sections, the boundary Γ can be divided into two parts: one perpendicular, $\Gamma_\perp$, and another one parallel to the direction of propagation, $\Gamma_\parallel$, illustrated in Fig. 1. For applications requiring the calculation
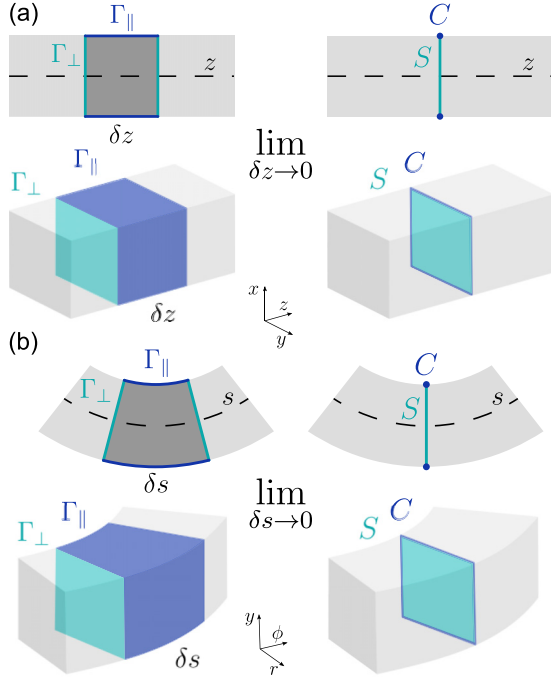
FIG. 1. Surface of integration for Eq. (8). In (a) we show the simple case of propagation in the z axis along infinite straight and parallel waveguides, whereas in (b) we present the case of a circular path in cylindrical coordinates, parametrized by the arc length s. Although a particular case, it can be used to approximate infinitesimal sections of most arbitrary curved paths. $\Gamma_{\parallel}$ and $\Gamma_{\perp}$ denote, respectively, surfaces parallel and perpendicular to the direction of propagation. In the limit where the thickness δs or δz of the bounded volume tends to zero, the surface $\Gamma_{\parallel}$ is transformed into the line C, whereas the surface $\Gamma_{\perp}$ becomes the surface S. The first rows of (a) and (b) show a view from the top, and the second rows show a perspective view.

of a static structure deformation profile, the knowledge of the total force is not enough, and the linear force density along the propagation direction, $\partial_s \mathbf{F}$, is also required. We parametrize the propagation direction by an arc length s so that curved waveguides can also be described with ease. To calculate $\partial_s \mathbf{F}$ we integrate Eq. (8) on a slice of infinitesimal thickness δs in the s axis and take the limit $\delta s \to 0$, as shown in Fig. 1(b). In this limit, the surfaces $\Gamma_{\perp}$ and $\Gamma_{\parallel}$ become the surface S and the line C, respectively, illustrated in Fig. 1. The force density on that slice becomes

$$\partial_s \mathbf{F} = \iint_S \langle \partial_s \mathcal{T}_{\text{in}} \rangle \cdot \hat{\mathbf{n}} \, dS + \iint_S \langle \mathcal{T}_{\text{in}} \rangle \cdot \partial_s \hat{\mathbf{n}} \, dS$$
$$+ \oint_C \langle \mathcal{T}_{\text{out}} \rangle \cdot \hat{\mathbf{n}} \, dl, \qquad (9)$$

where the first and second terms are integrated over the cross-section area S and the third term is a line integral over the boundary of C. On the surface S, the fields outside the domain of integration are the same as the fields inside it, since S lies entirely inside the dielectric. We rename the tensor in these cases as $\mathcal{T}_{\text{in}}$ to represent the fields inside matter to avoid confusion.

For eigenmodes propagating in the z axis, Fig. 1(a), we have $\partial_z \hat{\mathbf{n}} = 0$, since the normal in the cross section is not changing, and $\langle \partial_z \mathcal{T}_{\text{in}} \rangle = 0$, since for eigenmodes the stress tensor is z independent. In this specific case of eigenmodes propagating in a section of zero curvature, only the third integral in Eq. (9) survives and the force density $\partial_z \mathbf{F}$ is formulation independent, depending solely on the fields outside the dielectric. It is important to notice that we assume that $\varepsilon = 1$ outside the material, a situation in which Eq. (2) shows that all stress tensors will coincide with the Lorentz formulation. However, if the waveguides are surrounded by another dielectric material, different formulations lead to different predictions even for eigenmode forces.

Since the first and second term in Eq. (9) depend on the fields inside the material ($\mathcal{T}_{\text{in}}$), in a general scenario different force laws will result in different forces, as we have shown in a previous work, when studying the appearance of a beating force due to noneigenmode excitation [23]. In summary, a noneigenmode excitation have a non-null first term in Eq. (9), whereas a curved propagation has a non-null second term due to the varying normal. The third term in Eq. (9) will always be present, but on certain occasions it can be zero due to symmetries.

The quantity $\mathcal{T}_{nm} \cdot \hat{\mathbf{n}}$ in Eq. (9) plays a major role when analyzing the differences between force formulations. For the case of straight waveguides, $\hat{\mathbf{n}} = \hat{\mathbf{z}}$, it can be calculated as

$$\mathcal{T}_{nm}^E \cdot \hat{\mathbf{n}} = \varepsilon_0 \{ \varepsilon^n (\boldsymbol{\mathcal{E}} \cdot \hat{\mathbf{z}}) \boldsymbol{\mathcal{E}} - \tfrac{1}{2} \varepsilon^m (\boldsymbol{\mathcal{E}} \cdot \boldsymbol{\mathcal{E}}) \hat{\mathbf{z}} \}, \qquad (10)$$

where for simplicity only the electric-field dependent terms are shown since in nonmagnetic isotropic and linear dielectrics they are the only ones that change depending on the formulation. No time averaging is taken.

As can be seen from Eq. (10), the label m only changes the force in the z direction. Tensors with the same value of n, Lorentz and unnamed ($n = 0$), and Einstein-Laub and Minkowski ($n = 1$), will give the same prediction with respect to the transverse forces, but each tensor leads to a different force density along z.

The differences between the quantity $\mathcal{T}_{nm} \cdot \hat{\mathbf{n}}$ for different labels, and hence formulations, can help us understand the differences in the forces. We have that

$$(\mathcal{T}_{1m} - \mathcal{T}_{0m}) \cdot \hat{\mathbf{n}} = (\boldsymbol{\mathcal{P}} \cdot \hat{\mathbf{z}}) \boldsymbol{\mathcal{E}}, \qquad (11)$$

$$(\mathcal{T}_{n1} - \mathcal{T}_{n0}) \cdot \hat{\mathbf{n}} = -\tfrac{1}{2} (\boldsymbol{\mathcal{E}} \cdot \boldsymbol{\mathcal{P}}) \hat{\mathbf{z}}, \qquad (12)$$

where $\boldsymbol{\mathcal{P}}$ is the polarization. Equation (11) can be understood as the force on the surface bound charges while Eq. (12) is the energy stored in the dielectric media. It is worth noticing that no geometry or other constraint is used in the derivation of these equations besides the media being linear, therefore they are as general as possible in this context.

For the general case of curved waveguides, using the Frenet-Serret formulas it is possible to show that $\partial_s \hat{\mathbf{n}}$ is a vector in the cross-section plane. Therefore, there are terms dependent on n and m in the transverse and longitudinal directions. This results in all force laws giving different predictions for the force, even in the eigenmode case.
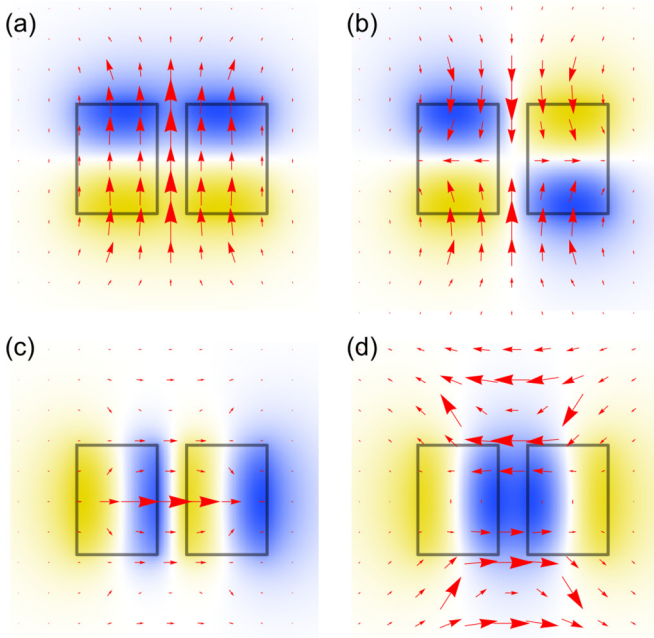
FIG. 2. Field profiles for the four eigenmodes of the system of coupled waveguides. Eigenmodes presented in (a)–(d) will be referred to as modes 1–4, respectively. The electric field perpendicular to the page (E_z) is presented in a color scale, where the color ranges from blue (dark gray) negative values to yellow (light gray) positive values, while the red arrows represent the in-plane electric field (E_x and E_y). Due to a freedom in defining the phase of the E_z component with respect to those of E_x and E_y, we have chosen to represent the phase of the total field for which E_z is purely imaginary and the transverse fields are purely real.

III. RESULTS AND DISCUSSION

In order to evaluate quantitatively the force laws presented in the previous section, we run simulations using the FEM with the commercial software COMSOL Multiphysics, for silicon waveguides with a refractive index of 3.45 at an excitation wavelength of 1550 nm. We model waveguides using a rectangular cross section with a width of 280 nm and height of 380 nm. For the single waveguide geometry (zero gaps) the width is 560 nm, while the height remains 380 nm. Curved sections are simulated using sectors of concentric rings with radii $(4 \pm \delta g/2)$ μm, δg being the gap between the waveguides. A nominal gap of 80 nm is used in the computations where the waveguide separation is not varied.

Figure 2 shows the electric-field profile for the coupled waveguides. Color data represent the electric field perpendicular to the page and the arrows show the in-plane electric field. The modes shown in Figs. 2(a) and 2(b) have a TE-like polarization and are referred to as mode 1 and 2, while modes 3 and 4 are shown in Figs. 2(c) and 2(d) and have a TM-like polarization.

We now proceed to present and discuss the results for straight coupled waveguides, with the monochromatic wave propagating along the z direction. Figure 3 shows the optical-force densities calculated using Eq. (9) for this geometry, normalized for input power, as a function of their separation. We have calculated the forces due to excitation by each
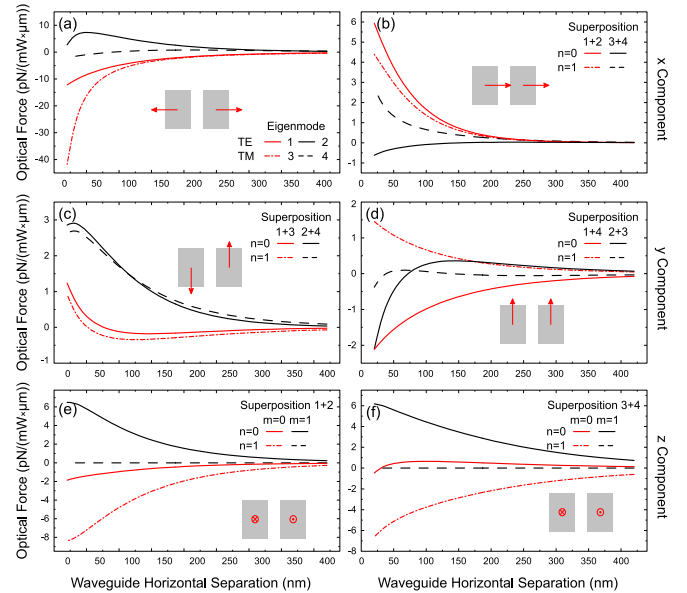

FIG. 3. Comparison of optical forces calculated using Eq. (9) for a pair of straight coupled waveguides sustaining four eigenmodes, two TE-like and two TM-like. Insets show the direction and sign of the force in each waveguide, and indicate to which mode superposition and value of n and m each curve corresponds. The four eigenmode forces are shown in (a). Since all force laws agree for eigenmodes, a single line is presented for each mode. For superpositions of eigenmodes, only the beating force components are shown in (b)–(f). The x component of the beating force, shown in (b), is present for mode superpositions $1 + 2$, red lines (light gray), and $3 + 4$, black lines. The y component presented in (c) and (d) is nonzero for mode superpositions $1 + 3$, $2 + 4$, $1 + 4$, and $2 + 3$. The longitudinal component, z, of the beating forces only appears for superpositions $1 + 2$ (e) and $3 + 4$ (f). For (b)–(d), only the n value of Eq. (2) is relevant, and the forces split in two groups of similar qualitative behavior, whereas in (e) and (f) there are four different longitudinal components, due to the dependence on both n and m. The inset shows how the force (red arrows) acts on different waveguides.

eigenmode individually, originating from the third term in Eq. (9), and by all possible superpositions of the four eigenmodes. For mode superpositions, only the additional beating force terms [originating from the first term in Eq. (9)] are plotted, as the third term of Eq. (9) is always present. Moreover, as the beating terms vary sinusoidally along z, only the amplitude of the forces is shown, for the sake of clarity.

Figure 3(a) shows the forces for the four eigenmodes on the system. These are attractive or repulsive forces, and have been known and studied since 2005 [24]. We present only one curve for each eigenmode as, for this particular case, all force laws produce the same result. This is simple to understand, since the third term of Eq. (9) uses only the stress tensor outside the material. Our simulations consider the dielectric waveguides to be suspended in vacuum, so all stress tensors reduce to the Lorentz one outside the waveguides. However, if the waveguides were not in vacuum but embedded in a different dielectric medium, the forces would differ even for the case of eigenmode excitation.

Figures 3(b)–3(f) show the different beating force components that can act on the system when different

superpositions of eigenmodes propagate through the waveguides. The combination of different symmetries yields forces not only in different directions but also with different characteristics. Figures 3(b) and 3(d) show the beating force acting on the center of mass of the cross section, whereas Figs. 3(c), 3(e) and 3(f) show it acting as a shear force (opposite sign on opposite waveguides, but orthogonal to the gap between them). The forces acting on the center of mass of the cross section are associated to an exchange of linear momentum due to a change in the transverse position of the center of energy of the light beam along the direction of propagation, as discussed in [23] for the x component shown in Fig. 3(b). For the case of the y component, this change is vertical, and therefore more limited, leading to smaller forces in Fig. 3(d).

The shear forces, however, are associated to torques on the structure, and therefore must correspond to exchanges of angular momentum. This connection should be kept in mind when we proceed to discuss how the different optical forces produce different predictions, in particular for the z shear force. It is worth noticing the y shear appears when eigenmodes of different polarization, but same xy parity, are combined. In this case the coupled waveguides act as an effective birefringent medium, introducing a rotation of the effective polarization of the beam which in turn leads to a torque on the material system, as observed by Beth on waveplates [25]. The z shear can be understood as originating from the loss of forward electromagnetic momentum in one guide and corresponding increase in the other. By taking the straight waveguides to be sections of arbitrarily large concentric rings, the z shear can also be understood as an exchange of orbital angular momentum.

Having discussed the general properties shared by all optical-force laws for a given mode superposition, we now compare the predictions from different optical-force laws. We begin by reiterating that for eigenmodes all force laws give the same result, as already proved. For the beating force, transverse components (x and y) shown in Figs. 3(b)–3(d) depend only on the value of n in Eq. (9), as was shown by expanding the general stress tensor in Eq. (10). The dependence only on n means that both the E-L and Minkowski forces give the same result, different from the Lorentz force. This means the unnamed force automatically agrees with the Lorentz force. Contrary to the transverse forces, the longitudinal beating force (z), shown in Figs. 3(e) and 3(f), depends on both n and m.

For the x force due to the superposition of modes 1 and 2 we find very little disagreement between the four force laws. It increases as the gap decreases, but the qualitative behavior is the same for both. When calculating the y shear we also find very little quantitative and qualitative disagreement for both mode superpositions, showing that while the E-L and Lorentz forces have fundamental differences on how they treat matter this has little impact on the predictions they offer for this particular angular momentum exchange.

Quantitative and qualitative differences are more marked for the $3 + 4$ [black curves in Fig. 3(b)], $1 + 4$, and $2 + 3$ [Fig. 3(d)] mode superpositions, where qualitative differences can also be noticed. In the case of the x force due to the superposition of two TM-like modes, not only does the Lorentz force law predict a weak force for most gaps, while the E-L

and Minkowski force laws predict a stronger force, but these predictions also have opposite signs. For the TE-like superposition the force laws are in good agreement. The most striking result, however, is that of the z component for superpositions $1 + 2$ and $3 + 4$, where each force law gives a different prediction. The Minkowski force law, in particular, predicts no force in this direction, even though there is a clear decrease in the linear momentum in the z direction for these cases.

Finally, we analyze the force terms due to the second term in Eq. (9), using a curved section of a single waveguide and of a pair of coupled waveguides. For this term each force law gives a different prediction, even in the case of eigenmodes. Presenting the results in the same manner used for straight sections is therefore not possible, as the number of optical-force densities grows drastically (there are 16 forces for eigenmodes alone instead of four). Instead, we choose to focus on the transverse x component of the Lorentz optical force for curved sections of single and double waveguides, and on how it changes along the direction of propagation, parametrized by an arc length. For double waveguides, the gap between waveguides is chosen to be 80 nm. Results are presented in Fig. 4, and for a better comparison we present results for straight (a)–(d) and curved (e)–(h) waveguides. We show eigenmode forces (a), (c), (e), (g) and the total force, which includes both beating and eigenmode terms, for a superposition of modes 1 and 2 (b), (d), (f), (h).

Due to the symmetry of the fields, the eigenmode force is zero for a single straight waveguide (a), whereas for a single curved waveguide (e) the eigenmodes can produce a force due to the changing linear momentum necessary for light to follow a curved path. A mode superposition results in a pure beating force term acting on the straight single waveguide (b), but the corresponding total force for the curved waveguide does not vary symmetrically from $+F$ to $-F$, due to the nonzero eigenmode force (f). It is well known that eigenmode forces for straight coupled waveguides (c) have equal modulus and opposite sign. This means that the total transverse force for a mode superposition is different on each waveguide, since the beating term has equal sign for both waveguides (d). The case of curved coupled waveguides is even richer. Eigenmode forces (g) do not have the same modulus on each waveguide, since each has a slightly different radius of curvature. The total force in a superposition (h) is not only asymmetrically shifted, however. The amplitude of the force is different in each waveguide and the sinusoidal modulations no longer are in phase or have the same period, due to the different radius of each waveguide.

IV. CONCLUSIONS

Even though classical electromagnetism has been under study for more than a century, some core issues remain open. One such issue is that of the correct force law to describe the action of optical fields on dielectric objects. While there is a growing consensus that the Lorentz, Minkowski, Abraham, and Einstein-Laub force laws are associated to incomplete descriptions of the field-material system, and that a proper force law can be derived from the total-energy-momentum tensor, these force laws are still widely used.
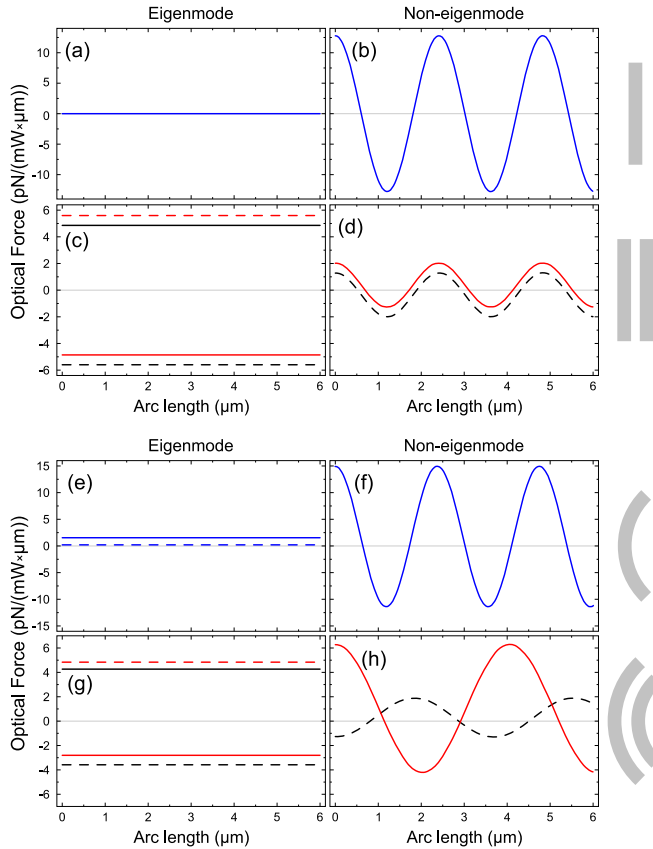
FIG. 4. Transverse optical forces (*x* direction) along the propagation direction for straight and curved sections of a single waveguide and a pair of waveguides. In (a), (b), (e), and (f) are shown results for a single waveguide, whereas (c), (d), (g), and (h) present results for a pair of coupled waveguides. The eigenmode forces are presented in (a), (c), (e), and (g), whereas (b), (d), (f), and (h) show the total force (eigenmode forces + beating force) in a mode superposition. Blue (light gray) curves represent forces in a single-waveguide scenario in (a), (b), (e), and (f), whereas red (light gray) and black curves represent the force on the left or right waveguide of a coupled pair in (c), (d), (g), and (h), respectively. In (a), (c), (e), and (g) solid lines indicate forces due to mode 1, and dashed lines indicate those due to mode 2. The inset on the right shows the waveguide configurations considered.

We have shown that for linear media the main computational difference is that all force regimes can be described either as a force acting on surface bound charges or as the energy stored in the dielectric media. With this formalism it becomes apparent what are the main distinctions of difference force laws.

We have used a pair of coupled waveguides supporting four global eigenmodes as a test system to study cases in which the force laws gave different predictions. Instead of directly using the force laws, we have constructed a general stress tensor that reduces to each of the well-known tensors by a choice of two binary parameters. We then used the momentum conservation equation to calculate the force density acting on the waveguide cross section, later obtaining the predictions from each force law by varying the parameters in the general tensor.

We have shown that a strict application of the divergence theorem, making no *a priori* symmetry assumptions, allows this equation to be broken into three distinct contributions, each related to different ways momentum can be transferred within the field-matter system. The first one is associated to the momentum of each eigenmode propagating in the system, and how it varies due to the change in dispersion when the gap between waveguides changes. The second is associated to how the transverse distribution of the total momentum varies along the direction of propagation for a superposition of eigenmodes, due to the different propagation constants, and gives rise to beating forces that are modulated along the direction of propagation. The third term depends on the curvature of the waveguides, since even eigenmodes propagating in a curved waveguide must suffer a change in the direction of their momentum to remain guided.

This method has allowed us to identify that predictions for transverse beating forces have large differences for certain mode superpositions and are almost identical for others. In particular we highlight the good agreement for the case of the *y* shear force associated to a rotation of the effective polarization of the guided fields, and the strong differences predicted for the *z* longitudinal beating force, which can be thought of in terms of orbital angular momentum transfer. Angular momentum has featured prominently in the discussion about stress tensors in dielectrics, and we intend to further investigate the *y* and *z* shears in light of the more recent idea of constructing an energy-momentum tensor that properly describes the full system.

Finally, we believe that this discussion should be followed by experimental tests since in some situations the predicted result is markedly different for each force law. We believe that it is important to first consider all four stress tensors when designing a device, as for some applications the differences will be inconsequential but for others they might prove to be critical. In addition to contributing to the ongoing discussion about optical forces in dielectrics, we believe that our contribution can also find applications in the design of integrated optomechanical devices, much in the same way as the inclusion of additional material effects in the modeling has lead to the design of new devices based on high photoelastic coupling instead of the so-called moving boundary coupling due to radiation pressure.

[1] M. Abraham, Rend. Circ. Mat. Palermo **28**, 1 (1909).

[2] W. D. Phillips and H. Metcalf, Phys. Rev. Lett. **48**, 596 (1982).

[3] A. Ashkin, J. M. Dziedzic, and T. Yamane, Nature (London) **330**, 769 (1987).

[4] P. Y. Chiou, A. T. Ohta, and M. C. Wu, Nature (London) **436**, 370 (2005).

[5] R. N. C. Pfeifer, T. A. Nieminen, N. R. Heckenberg, and H. Rubinsztein-Dunlop, Rev. Mod. Phys. **79**, 1197 (2007).

[6] M. Mansuripur, Opt. Commun. **283**, 1997 (2010).

[7] T. Ramos, G. F. Rubilar, and Y. N. Obukhov, Phys. Lett. A **375**, 1703 (2011).

[8] B. A. Kemp, J. Appl. Phys. **109**, 111101 (2011).

[9] M. Mansuripur, Opt. Express **16**, 14821 (2008).

[10] A. R. Zakharian, P. Polynkin, M. Mansuripur, and J. V. Moloney, Opt. Express **14**, 3660 (2006).

[11] M. Mansuripur, A. R. Zakharian, and E. M. Wright, Phys. Rev. A **88**, 023826 (2013).

[12] A. M. Jazayeri and K. Mehrany, Phys. Rev. A **89**, 043845 (2014).

[13] H. Rubinsztein-Dunlop, A. Forbes, M. V. Berry, M. R. Dennis, D. L. Andrews, M. Mansuripur, C. Denz, C. Alpmann, P. Banzer, T. Bauer, E. Karimi, L. Marrucci, M. Padgett, M. Ritsch-Marte, N. M. Litchinitser, N. P. Bigelow, C. Rosales-Guzmán, A. Belmonte, J. P. Torres, T. W. Neely, M. Baker, R. Gordon, A. B. Stilgoe, J. Romero, A. G. White, R. Fickler, A. E. Willner, G. Xie, B. McMorran, and A. M. Weiner, J. Opt. **19**, 013001 (2017).

[14] E. Li, B. J. Eggleton, K. Fang, and S. Fan, Nat. Commun. **5**, 3225 (2014).

[15] R. Van Laer, B. Kuyken, D. Van Thourhout, and R. Baets, Nat. Photonics **9**, 199 (2015).

[16] E. Ippen and R. Stolen, Appl. Phys. Lett. **21**, 539 (1972).

[17] H. Shin, W. Qiu, R. Jarecki, J. A. Cox, R. H. Olsson, A. Starbuck, Z. Wang, and P. T. Rakich, Nat. Commun. **4**, 1944 (2013).

[18] T. Požar, J. Laloš, A. Babnik, R. Petkovšek, M. Bethune-Waddell, K. J. Chau, G. V. B. Lukasievicz, and N. G. C. Astrath, Nat. Commun. **9**, 3340 (2018).

[19] J. D. Jackson, *Classical Electrodynamics*, 3rd ed. (Wiley, New York, 1998).

[20] M. Negahban, *Continuum*, 1st ed. (CRC, Boca Raton, FL, 2005).

[21] A. R. Khoei, *Extended Finite Element Method: Theory and Applications*, 1st ed. (Wiley, New York, 2015).

[22] B. A. Kemp, T. M. Grzegorczyk, and J. A. Kong, Opt. Express **13**, 9280 (2005).

[23] T. F. D. Fernandes, C. M. K. C. Carvalho, P. S. S. Guimaraes, B. R. A. Neves, and P.-L. de Assis, J. Lightwave Technol. **36**, 1608 (2018).

[24] M. L. Povinelli, M. Lončar, M. Ibanescu, E. J. Smythe, S. G. Johnson, F. Capasso, and J. D. Joannopoulos, Opt. Lett. **30**, 3042 (2005).

[25] R. A. Beth, Phys. Rev. **50**, 115 (1936).